ACS Photonics

Letter

pubs.acs.org/journal/apchd5

# Temperature-Dependent Photoluminescence Characteristics of GeSn Epitaxial Layers

Fabio Pezzoli,*[,†] Anna Giorgioni,[†] David Patchett,[‡] and Maksym Myronov*[,‡]

[†]LNESS and Dipartimento di Scienza dei Materiali, Università di Milano-Bicocca, Via R. Cozzi 55, 20125 Milano, Italy

[‡]Department of Physics, The University of Warwick, Coventry CV4 7AL, United Kingdom

Supporting Information

**ABSTRACT:** $Ge_{1-x}Sn_x$ epitaxial heterostructures are emerging as prominent candidates for the monolithic integration of light sources on Si substrates. Here we propose a suitable explanation for their temperature-dependent photoluminescence (PL) that is based upon the so far disregarded optical activity of dislocations. By working at the onset of plastic relaxation, which occurs whenever the epilayer releases the strain accumulated during growth on the lattice-mismatched substrate, we demonstrate that dislocation nucleation can be explicitly seen in the PL data. Notably, our findings point out that a monotonic thermal PL quenching can be observed in coherent films, in spite of the indirect nature of the $Ge_{1-x}Sn_x$ band-gap. Our investigation, therefore, contributes to a deeper understanding of the recombination dynamics in this intriguing group IV alloy and offers insights into crucial phenomena shaping the light emission efficiency.

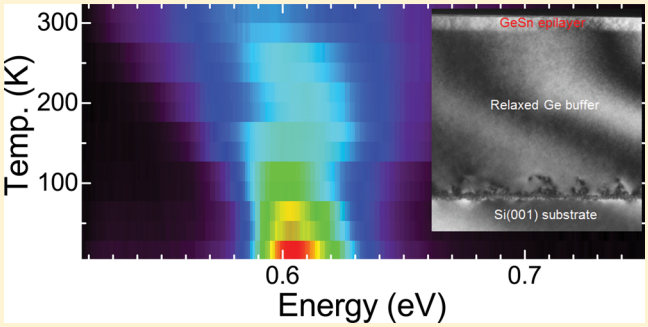


**KEYWORDS:** *GeSn, germanium, dislocations, strain, photoluminescence, RP-CVD*

The recently discovered lasing action in $Ge_{1-x}Sn_x$,[1] tensile-strained Ge,[2,3] and nanostructured[4] Ge has sparked the quest for identifying group IV candidates boasting a direct band-gap. Their monolithic integration on Si holds the promise to revolutionize information technology by spurring the wafer-scale establishment of advanced photonic circuits.[5] Arguably, light routing into the cost-effective Si platform has applications beyond communication, including biological sensing,[6,7] optical memories,[8,9] and quantum computation.[10−12]

Despite the remarkable progress in heteroepitaxy and fabrication techniques that made strain and band-gap engineering readily available, the contrasting theoretical[13−15] and experimental[1,16−18] data accumulated in the literature proved the crucial resolution of the indirect-to-direct crossover to be nontrivial and highly debated in semiconductors based on group IV materials.

The increase of the photoluminescence (PL) intensity with decreasing temperature has been recently put forward as a compelling proof that the fundamental energy gap of $Ge_{1-x}Sn_x$ binary alloys can be direct in the momentum space.[1] Since this method is now increasingly applied,[19−23] we find it crucial to examine the possible pitfalls associated with it. Indeed, the PL intensity is, to a good approximation, proportional to the quantum efficiency, thus prone to the entangled interplay between all the possible radiative and nonradiative processes. While the PL enhancement with decreasing temperature can be intuitively associated with direct band-gap semiconductors, which entail III−V compounds and transition metal dichalcogenide monolayers as well-cited examples, under suitable conditions it can unexpectedly occur also in indirect band-gap materials[24] including Ge.[25−28]

In this work, we demonstrate that a detailed knowledge of the recombination dynamics at ubiquitous defects, namely, dislocations, is pivotal for a correct physical interpretation of the measured temperature dependence of the PL. Notably, despite evidence that is arising for defect-related Shockley−Read−Hall recombination in group IV heterostructures,[1,29] very little is known about the nature and the optical activity of defects, chiefly dislocations. Understanding such phenomena is indeed of prime interest for overcoming the stringent roadblocks in the achievement of efficient lasing operation at room temperature.

To tackle this challenge, we focus on ultrathin $Ge_{1-x}Sn_x$ epitaxial layers grown on Ge-buffered Si substrates. By deliberately exploiting alloys with a Sn content below 9%,[1] we restrict ourselves to indirect gap materials and leverage their optical response as very sensitive probes of the defect-assisted recombination and generation of the photogenerated carriers. Notably, varying the epilayer thickness at the threshold of plastic relaxation for a given Sn content allows us to selectively inhibit dislocation nucleation and provides us with a small and adjustable strain relaxation. By doing so, we are well-positioned to explore how dislocations affect recombination dynamics through the opening of parasitic nonradiative recombination channels.

**Received:** June 27, 2016
**Published:** October 17, 2016





DOI: 10.1021/acsphotonics.6b00438
*ACS Photonics* 2016, 3, 2004−2009

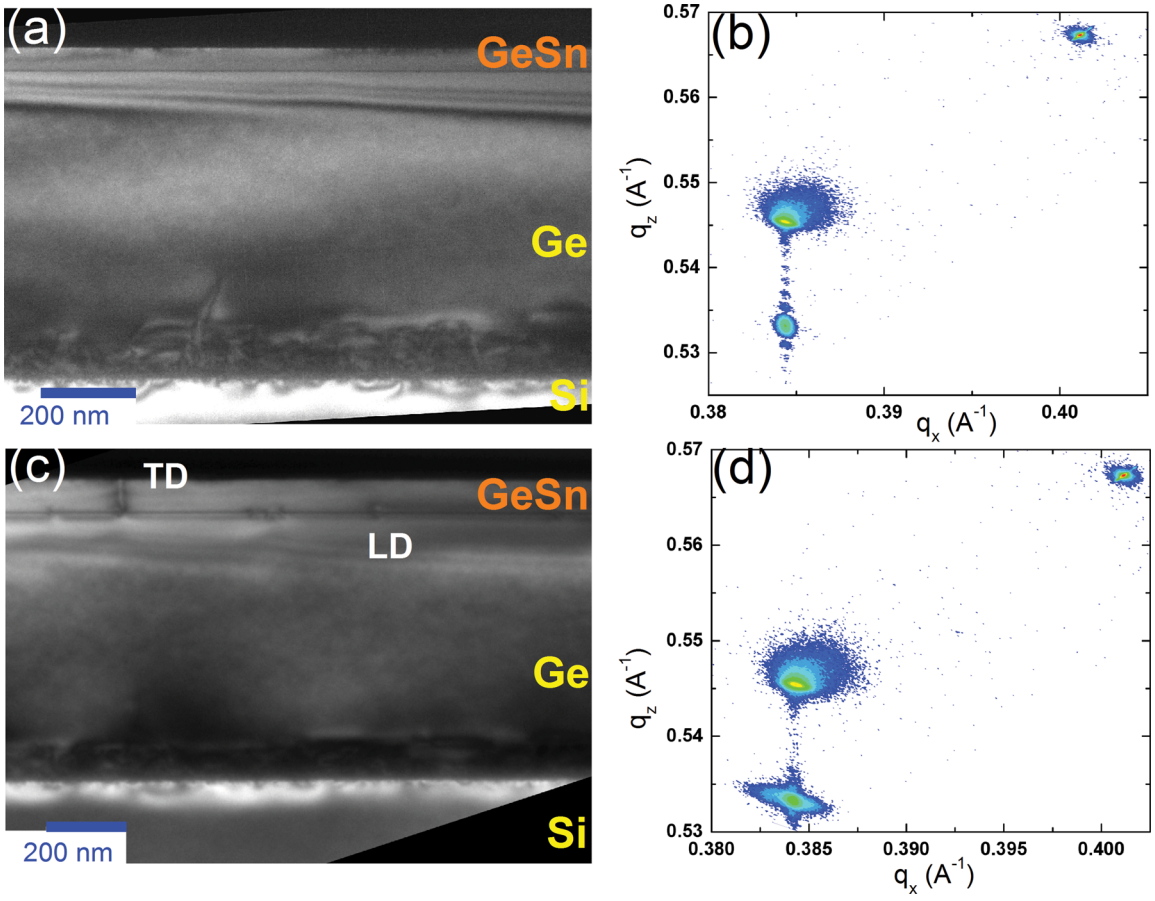


**Figure 1.** (a) Cross-sectional TEM image and (b) asymmetric (224) reciprocal space map of the fully strained $Ge_{0.91}Sn_{0.09}$/Ge/Si heterostructure. (c and d) TEM and X-ray data of a $Ge_{0.91}Sn_{0.09}$ epilayer having a strain relaxation of 6%. The silicon substrate, the Ge buffer layer, and the GeSn film are indicated alongside 90° Lomer dislocations (LD) and threading dislocation (TD) arms related to 60° dislocations.

For this work the $Ge_{1-x}Sn_x$ epilayers of various Ge content and thickness were grown on an 100 mm diameter Si(001) substrate via an intermediate relaxed Ge buffer layer to minimize the lattice mismatch, and consequently the compressive strain, between the $Ge_{1-x}Sn_x$ epilayer and the Si substrate. It should be noted that just a ~650 nm thick relaxed Ge buffer produces a very high quality surface for the $Ge_{1-x}Sn_x$ heteroepitaxy with a root-mean-square surface roughness below 1 nm and a threading dislocation density (TDD) below $10^7$ $cm^{-2}$. The structures were grown using an industrial type ASM Epsilon 2000 reduced pressure chemical vapor deposition (RP-CVD) reactor with commercially available precursors digermane ($Ge_2H_6$) and tin-tetrachloride ($SnCl_4$) diluted in hydrogen. The epitaxial growth was carried out in a hydrogen atmosphere and at a reduced pressure below 100 Torr. The samples were not intentionally doped. The residual background doping was estimated to be a few $10^{15}$ $cm^{-3}$ for the GeSn epilayers and below $10^{15}$ $cm^{-3}$ in the buffer. The thicknesses of the $Ge_{1-x}Sn_x$ films were obtained by analysis of cross-sectional transmission electron microscopy (TEM) images, while the Sn fractions and the state of strain were obtained from analysis of symmetrical (004) and asymmetrical (224) high-resolution X-ray diffraction (HR-XRD) reciprocal space maps. The TEM image in Figure 1a demonstrates that for a $Ge_{1-x}Sn_x$ thickness of ~40 nm the $Ge_{0.91}Sn_{0.09}$/Ge heterointerface retains a perfect crystalline quality and is free from extended defects. It should be noted, however, that threading dislocations, originated at the buried Ge/Si interface, pierce through the buffer and might still be present in the topmost $Ge_{1-x}Sn_x$ layer, even though none is visible in the field of view of Figure 1a. The HR-XRD reciprocal space map measured around the asymmetric (224) reflection is shown in Figure 1b and demonstrates the attained coherent growth condition; that is, the $Ge_{0.91}Sn_{0.09}$ film is under compressive strain and coherent with the underlying Ge buffer. Figure 1c and d, however, elucidate that strain relaxation can occur as the $Ge_{0.91}Sn_{0.09}$ thickness is increased. The strain relief drives a sizable injection at the $Ge_{0.91}Sn_{0.09}$/Ge interface of extended defects, mainly in the form of Lomer 90° dislocations. Table 1 provides a survey of the structural parameters of all the $Ge_{1-x}Sn_x$ samples utilized in this work.

**Table 1. Sn Content and Thickness of the $Ge_{1-x}Sn_x$ Samples Investigated in This Work: $R$ and $\epsilon$ Are the Values Experimentally Determined from X-ray Data for the Strain Relaxation and the Biaxial Strain, Respectively, and the Linear Dislocation Density, $\delta$, of 90° Dislocations Has Been Derived from the Analysis of Various TEM Images**

| Sn content (%) | thickness (nm) | $R$ (%) | $\delta$ ($\mu m^{-1}$) | $\epsilon$ (%) |
|---|---|---|---|---|
| 5 | 70 | 0 | 0 | −0.80 |
| 5 | 100 | 11.5 | 4 | −0.57 |
| 9 | 40 | 0 | 0 | −1.18 |
| 9 | 70 | 0.6 | 0.59 | −1.15 |
| 9 | 80 | 6 | 2.28 | −1.12 |



DOI: 10.1021/acsphotonics.6b00438
ACS Photonics 2016, 3, 2004−2009

To gain insight into the optical properties of $Ge_{1-x}Sn_x$ epitaxial layers, PL measurements were carried out using a closed-cycle variable-temperature cryostat. The samples were excited at 1.165 eV (1064 nm) by using a Nd-$YVO_4$ laser. The optically pumped surface area had an approximately circular shape with a diameter of ~40 $\mu$m, which resulted in a power density of a few kW/cm$^2$. The PL was analyzed by a monochromator equipped with an InGaAs detector having a cutoff at ~0.5 eV and double-checked by a Fourier transform spectrometer coupled to a PbS detector (cutoff at ~0.4 eV). In the former case, the PL spectra were numerically cleaned to remove the overlap with the second-order peak due to the incomplete rejection of the pump.

We begin by focusing on the optical properties of the samples with the highest Sn content. Figure 2a demonstrates

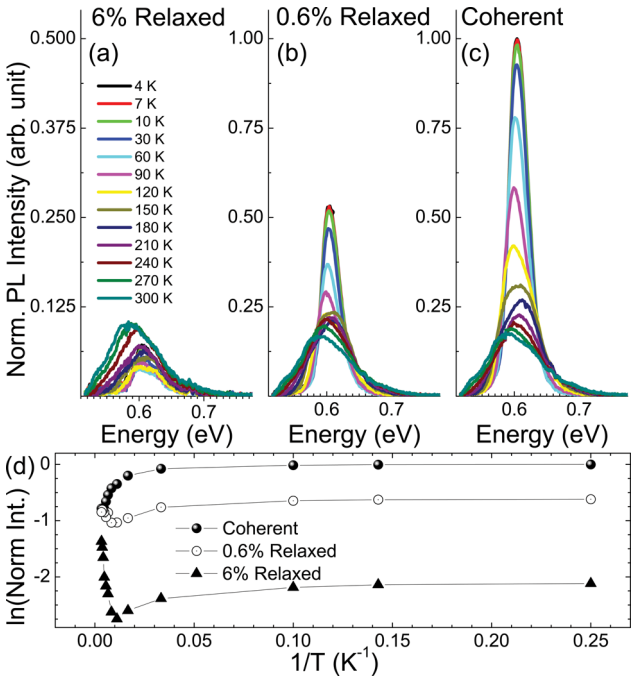


**Figure 2.** Photoluminescence (PL) spectra as a function of the temperature for $Ge_{0.91}Sn_{0.09}$ layers epitaxially grown on Ge-buffered Si(001) substrates. According to X-ray diffraction measurements, the epilayers are either partially relaxed with a relaxation degree of 6% (a) and 0.6% (b) or (c) fully strained, being grown coherently with the substrate. (d) Arrhenius plot summarizing the temperature dependence of the integrated PL intensity for the 6% (triangles) and 0.6% (open dots) partially relaxed and coherent (full dots) films. All the data are normalized to the low-temperature emission intensity of the coherent $Ge_{0.91}Sn_{0.09}$ sample.

the temperature-dependent PL of the sample capped with the partially relaxed $Ge_{0.91}Sn_{0.09}$ film. The peak at ~0.6 eV is attributed to the interband optical transitions occurring in the topmost $Ge_{1-x}Sn_x$ alloy layer. In line with the expected Ge-like band structure, deformation potential theory suggests that the low-temperature PL is dominated by the indirect band-gap recombination involving conduction band electrons at the *L*-point of the Brillouin zone and valence band heavy holes (HH) at the zone center (see Supporting Information). The built-in compressive strain removes the HH degeneracy with the light hole (LH) band, yielding a HH−LH separation of ~100 meV.[30,31] This strain-induced splitting and the weak dipole matrix element[32] conceal the observation of high-energy features due to transitions involving LH states at any of the pump power densities employed in this work (see Supporting Information).

Figure 2 shows that the PL signal turns out to be sizable up to room temperature, despite the overall reduced thickness of the $Ge_{1-x}Sn_x$/Ge stack and the complete absence of any surface passivation. On the other hand, at low temperature the PL intensity increases by decreasing the relaxation degree (Figure 2b,c). Eventually, the thinnest and fully strained $Ge_{0.91}Sn_{0.09}$ counterpart demonstrates the brightest emission (Figure 2c), a result that already discloses that the attained coherent growth suppresses nonradiative bulk-like recombination pathways, whose role, in addition, can be inferred to be prominent over the competing channel offered by the surface states.

It should be noted that no PL from the underlying Ge buffer was observed at the typical emission energies of Ge-on-Si heterostructures in the range from 0.6 to 0.9 eV.[28] The vast majority of radiative recombination events occurring in the $Ge_{1-x}Sn_x$ layer are thus likely to be due to its strong light absorption and the favorable $Ge_{1-x}Sn_x$/Ge band-edge alignment along with the poorest optical quality of the defective Ge buffer.

By increasing the temperature, the PL features experience a well-known red-shift[31,33] as a result of the band-gap shrinking (see also Supporting Information for a detailed discussion), while the concomitant integrated PL intensity discloses a nontrivial temperature behavior that differs drastically for the three $Ge_{0.91}Sn_{0.09}$ epilayers. Figure 2d surprisingly unveils that the coherent indirect $Ge_{1-x}Sn_x$ film demonstrates the simple monotonic PL quenching commonly argued to pertain to direct band-gap materials. Furthermore, the other two partially relaxed samples exhibit a puzzling surge of the PL intensity at lattice temperatures higher than 90 K ($T^{-1} \approx 1.1 \times 10^{-2}$ K$^{-1}$). Interestingly, such a steep increase gains a larger dynamic range by increasing the strain relaxation. We emphasize that the three $Ge_{0.91}Sn_{0.09}$ epitaxial layers differ solely in the thickness, in other words in the strain. Furthermore, the use of samples at the onset of plastic relaxation guarantees a gentle strain relief, which does not lead to appreciable deviations from the electronic band structure pertaining to the coherent, undoped $Ge_{1-x}Sn_x$ epilayer (see Supporting Information). This demonstrates that the remarkable distinction in terms of temperature characteristics, shown in Figure 2 under the same generation rate, stems from the activated optical activity of the dislocations injected in the two thickest samples through the plastic strain relaxation, and eventually it rules out competitive culprits such as the thermal activation of the background impurities.

The results summarized in Figure 2d for the partially relaxed samples compare well with recent reports about the optical properties of Ge/Si epitaxial architectures[28,34] and prove that in Ge-rich $Ge_{1-x}Sn_x$ alloys the defect-assisted recombination obeys the Schön−Klasens thermal mechanisms.[35] We can therefore rationalize the physical processes leading to the results of Figure 2 by considering the following scenario. At low temperatures, carriers photogenerated in indirect band-gap $Ge_{1-x}Sn_x$ alloys can be efficiently trapped at dislocations, if present, because their energy levels lie within the band-gap of the host semiconductor. Above a certain critical temperature, however, the thermal activation of trapped carriers occurs, eventually strengthening the radiative interband recombination, as experimentally observed in Figure 2b for the dislocated samples.



DOI: 10.1021/acsphotonics.6b00438
*ACS Photonics* 2016, 3, 2004−2009

In light of these findings, we point out that the measurement of the temperature-dependent PL characteristics as a function of the epilayer thickness, and specifically the rise of the band-edge recombination, can provide a sensitive spectroscopic method for the determination in undoped samples of the critical thickness above which dislocation nucleation is energetically favorable compared to the elastic energy accumulation in the growing film. This is of central importance for the ultimate fabrication of devices relying on heteroepitaxy on lattice-mismatched substrates.

A closer look at the PL data of Figure 2 provides us with additional information about the recombination pathways introduced by the defects in the $Ge_{1-x}Sn_x$ alloys. The weak emission intensity at the low-energy side of the main PL peaks is in line with literature reports about CVD samples[1] and makes the experimental investigation of the defect-assisted carrier dynamics more subtle and challenging than in pure Ge heterostructures. This elemental semiconductor belongs to the vast class of semiconductors governed by the Schön–Klasens mechanisms,[28,35] where a defect-related PL peak can often be observed and its measurable temperature-dependent quenching is accompanied by a coincident rise of other PL features.[28] It is therefore tempting to conceive that in $Ge_{1-x}Sn_x$ alloys the suppression of the dislocation-related PL might originate from the peculiar nature of the electronic states therein associated with the extended defects. Indeed our structural data are in line with available literature reports[1,29] and suggest the prominence of the 90° dislocations, which are less common than the 60° dislocations typically distinguished in Ge-based heterostructures.

It is worth noticing that another consistent explanation can be put forward for the low emission efficiency of the defect-related PL. By alloying Ge with Sn, the offset between the direct and indirect conduction band minima decreases. The more direct-like character of the band structure of $Ge_{1-x}Sn_x$ compared to that of Ge is expected to shorten the radiative lifetime. Under this condition, the interband transitions become more probable, and consequently the radiative recombination through the band-edges can increase at the expenses of the carrier recombination events, including radiative ones, taking place at the dislocation sites.

These arguments, the energy proximity of the defect-related PL with the cut-offs of our detectors, and the low dislocation density associated with the weak strain relaxation explored here (see Table 1) call for dedicated and systematic investigations, presently beyond the scope of this work, aimed at the experimental determination of the minority lifetimes in the binary alloy system and at a better theoretical understanding of the so-far elusive electronic states of defects in group IV semiconductors.

In the following, we further substantiate our assertion that the measurement of the temperature-dependent PL, and thereby the recombination dynamics, is strongly affected by the presence of optically active dislocations. To this purpose, we consider the set of indirect band-gap $Ge_{1-x}Sn_x$ heterostructures having the lowest Sn content, namely, 5% (see Table 1).

A direct comparison between Figure 2 and Figure 3 elucidates that the $Ge_{0.95}Sn_{0.05}$ epilayers fully recover the optical properties previously discussed for the Sn-richer $Ge_{0.91}Sn_{0.09}$ heterostructures. In particular, the temperature characteristic again demonstrates a net monotonic PL quenching as the thickness of the topmost $Ge_{1-x}Sn_x$ alloy layer is reduced so that coherent growth is satisfied and plastic relaxation is inhibited. In the partially relaxed Ge-rich $Ge_{0.95}Sn_{0.05}$ epilayer, a defect-related PL, albeit very weak, can be observed in the low-temperature regime at about 0.58 eV (see Figure 3a). Such defect-related transition exhibits a temperature-induced quenching that is consistent with the physical picture of the defect-mediated carrier dynamics, thus providing a compelling confirmation that the PL characteristics are substantially dictated by the presence of dislocations.

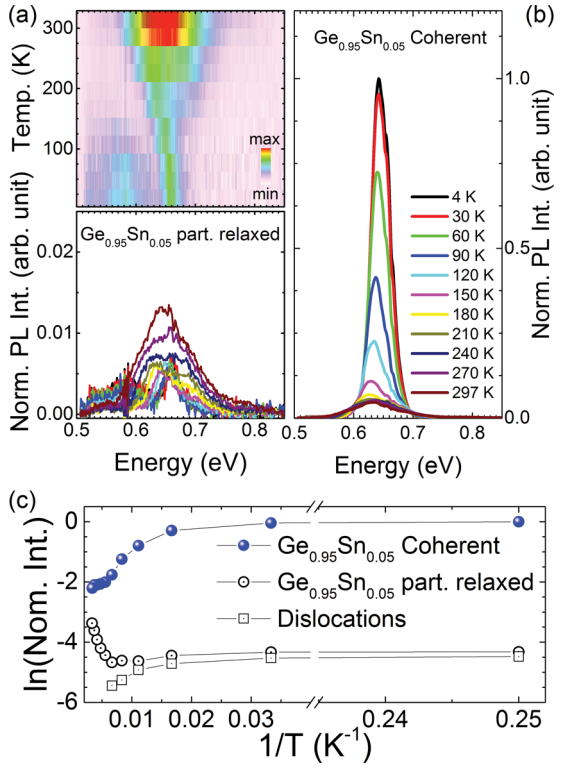


**Figure 3.** (a) Color-coded map of the temperature-dependent photoluminescence (PL) intensity (upper panel) and corresponding spectra (lower panel) for a partially relaxed $Ge_{0.95}Sn_{0.05}$ layer epitaxially grown on a Ge-buffered Si(001) substrate. (b) PL spectra as a function of the temperature for a fully strained coherent $Ge_{0.95}Sn_{0.05}$ layer. (c) Arrhenius plot summarizing the temperature dependence of the integrated PL intensity for the coherent (full dots) and partially relaxed (open dots) films. The open squares refer to the defect-related emission observed in the latter sample. All the data are normalized to the low-temperature emission intensity of the coherent $Ge_{0.95}Sn_{0.05}$ sample.

Figure 3c shows final intriguing phenomena. The integrated PL intensity of the partially relaxed $Ge_{0.95}Sn_{0.05}$ epilayer attains a minimum value at a temperature of about 120 K ($T^{-1} \approx 8 \times 10^{-3}$ $K^{-1}$), thus higher than what was obtained for the dislocated $Ge_{0.91}Sn_{0.09}$ samples. The increase of such critical temperature with a decrease in Sn content reflects the concomitant increase of the band-gap amplitude, a finding that naturally arises in the framework of rate equations modeling the capture and thermal release of carriers by the charged defect lines.[28,36]

In conclusion, by studying the temperature-dependent PL of indirect band-gap $Ge_{1-x}Sn_x$ epitaxial layers in the vicinity of the plastic strain relief, we were able to gather direct insights into the optical activity of growth defects, namely, dislocations. The unveiled pivotal role of dislocations on the recombination dynamics suggests that steady-state PL measurements need to


DOI: 10.1021/acsphotonics.6b00438
ACS Photonics 2016, 3, 2004–2009

be complemented by the direct measurements of the carrier lifetime in order to precisely resolve the directness of the electronic band structure. Our experimental findings can guide and stimulate novel theoretical investigations of the electronic structures of dislocations in Ge-based heterostructures, eventually providing a deeper understanding of existing and future experiments. Finally, in view of practical applications, we anticipated an advanced contactless spectroscopic technique to pinpoint dislocation injection in lattice-mismatched heteroepitaxy.

## ■ ASSOCIATED CONTENT

### Supporting Information

The Supporting Information is available free of charge on the ACS Publications website at DOI: 10.1021/acsphotonics.6b00438.

Electronic band structure and excitation power density dependence of the photoluminescence (PDF)

## ■ AUTHOR INFORMATION


### Corresponding Authors

*E-mail: fabio.pezzoli@unimib.it.

*E-mail: m.myronov@warwick.ac.uk.


### Notes

The authors declare no competing financial interest.

## ■ ACKNOWLEDGMENTS

The authors thank E. Vitiello and S. De Cesari for technical assistance and M. Guzzi and E. Grilli for fruitful discussions. This work was supported by the Fondazione Cariplo through Grant No. 2013.0623.

## ■ REFERENCES


(1) Wirths, S.; Geiger, R.; von den Driesch, N.; Mussler, G.; Stoica, T.; Mantl, S.; Ikonic, Z.; Luysberg, M.; Chiussi, S.; Hartmann, J. M.; Sigg, H.; Faist, J.; Buca, D.; Grützmacher, D. Lasing in direct-bandgap GeSn alloy grown on Si. *Nat. Photonics* **2015**, *9*, 88−92.

(2) Liu, J.; Sun, X.; Camacho-Aguilera, R.; Kimerling, L. C.; Michel, J. Ge-on-Si laser operating at room temperature. *Opt. Lett.* **2010**, *35*, 679.

(3) Camacho-Aguilera, R. E.; Cai, Y.; Patel, N.; Bessette, J. T.; Romagnoli, M.; Kimerling, L. C.; Michel, J. An electrically pumped germanium laser. *Opt. Express* **2012**, *20*, 11316−11320.

(4) Grydlik, M.; Hackl, F.; Groiss, H.; Glaser, M.; Halilovic, A.; Fromherz, T.; Jantsch, W.; Schäffler, F.; Brehm, M. Lasing from Glassy Ge Quantum Dots in Crystalline Si. *ACS Photonics* **2016**, *3*, 298.

(5) Liang, D.; Bowers, J. E. Recent progress in lasers on silicon. *Nat. Photonics* **2010**, *4*, 511.

(6) Chow, E.; Grot, A.; Mirkarimi, L. W.; Sigalas, M.; Girolami, G. Ultracompact biochemical sensor built with two-dimensional photonic crystal microcavity. *Opt. Lett.* **2004**, *29*, 1093−1095.

(7) Soref, R. Mid-infrared photonics in silicon and germanium. *Nat. Photonics* **2010**, *4*, 495−497.

(8) Ferrera, M.; Park, Y.; Razzari, L.; Little, B. E.; Chu, S. T.; Morandotti, R.; Moss, D. J.; Azaña, J. On-chip CMOS-compatible all-optical integrator. *Nat. Commun.* **2010**, *1*, 29.

(9) Ríos, C.; Stegmaier, M.; Hosseini, P.; Wang, D.; Scherer, T.; Wright, C. D.; Bhaskaran, H.; Pernice, W. H. P. Integrated all-photonic non-volatile multi-level memory. *Nat. Photonics* **2015**, *9*, 725.

(10) Politi, A.; Cryan, M. J.; Rarity, J. G.; Yu, S.; O'Brien, J. L. Silica-on-Silicon Waveguide Quantum Circuits. *Science* **2008**, *320*, 646−649.

(11) O'Brien, J. L.; Furusawa, A.; Vučković, J. Photonic quantum technologies. *Nat. Photonics* **2009**, *3*, 687.

(12) Shadbolt, P.; Mathews, J. C. F.; Laing, A.; O'Brien, J. L. Testing foundations of quantum mechanics with photons. *Nat. Phys.* **2014**, *10*, 278.

(13) Fitzgerald, E. A.; Freeland, P. E.; Asom, M. T.; Lowe, W. P.; Macharrie, R. A.; Weir, B. E.; Kortan, A. R.; Thiel, F. A.; Xie, Y. H.; Sergent, A. M.; Cooper, S. L.; Thomas, G. A.; Kimerling, L. C. Epitaxially stabilized GeSn diamond cubic alloys. *J. Electron. Mater.* **1991**, *20*, 489.

(14) He, G.; Atwater, H. A. Interband Transitions in SnxGe1-x Alloys. *Phys. Rev. Lett.* **1997**, *79*, 1937.

(15) Moontragoon, P.; Ikonić, Z.; Harrison, P. Band structure calculations of SiGeSn alloys: achieving direct band gap materials. *Semicond. Sci. Technol.* **2007**, *22*, 742.

(16) Ryu, M.-Y.; Harris, T. R.; Yeo, Y. K.; Beeler, R. T.; Kouvetakis, J. Temperature-dependent photoluminescence of Ge/Si and Ge1-ySny/Si, indicating possible indirect-to-direct bandgap transition at lower Sn content. *Appl. Phys. Lett.* **2013**, *102*, 171908.

(17) Ghetmiri, S. A.; Du, W.; Margetis, J.; Mosleh, A.; Cousar, L.; Conley, B. R.; Domulevicz, L.; Nazzal, A.; Sun, G.; Soref, R. A.; Tolle, J.; Li, B.; Naseem, H. A.; Yu, S.-Q. Direct-bandgap GeSn grown on silicon with 2230nm photoluminescence. *Appl. Phys. Lett.* **2014**, *115*, 151109.

(18) Gallagher, J. D.; Senaratne, C. L.; Kouvetakis, J.; Meendez, J. Compositional dependence of the bowing parameter for the direct and indirect band gaps in Ge1-ySny alloys. *Appl. Phys. Lett.* **2014**, *105*, 142102.

(19) Stange, D.; Wirths, S.; von den Driesch, N.; Mussler, G.; Stoica, T.; Ikonic, Z.; Hartmann, J. M.; Mantl, S.; Grützmacher, D.; Buca, D. Optical Transitions in Direct-Bandgap Ge1-xSnx Alloys. *ACS Photonics* **2015**, *2*, 1539−1545.

(20) Virgilio, M.; Schroeder, T.; Yamamoto, Y.; Capellini, G. Radiative and non-radiative recombinations in tensile strained Ge microstrips: Photoluminescence experiments and modeling. *J. Appl. Phys.* **2015**, *118*, 233110.

(21) Kurdi, M. E.; Prost, M.; Ghrib, A.; Sauvage, S.; Checoury, X.; Beaudoin, G.; Sagnes, I.; Picardi, G.; Ossikovski, R.; Boucaud, P. Direct Band Gap Germanium Microdisks Obtained with Silicon Nitride Stressor Layers. *ACS Photonics* **2016**, *3*, 443−448.

(22) Biswas, S.; Doherty, J.; Saladukha, D.; Ramasse, Q.; Majumdar, D.; Upmanyu, M.; Singha, A.; Ochalski, T.; Morris, M. A.; Holmes, J. D. Non-equilibrium induction of tin in germanium: towards direct bandgap Ge1-xSnx nanowires. *Nat. Commun.* **2016**, *7*, 11405.

(23) Geiger, R., Zabel, T., Marin, E., Gassenq, A., Hartmann, J.-M., Widiez, J., Escalante, J., Guilloy, K., Pauc, N., Rouchon, D., Osvaldo Diaz, G., Tardif, S., Rieutord, F., Duchemin, I., Niquet, Y.-M., Reboud, V., Calvo, V., Chelnokov, A., Faist, J., Sigg, H. *Uniaxially stressed germanium with fundamental direct band gap*. *arXiv:1603.03454*.

(24) Klein, P. B.; Nwagwu, U.; Edgar, J. H.; Freitas, J. A. J. Photoluminescence investigation of the indirect band gap and shallow impurities in icosahedral B12As2. *J. Appl. Phys.* **2012**, *112*, 013508.

(25) Wan, J.; Jin, G. L.; Jiang, Z. M.; Luo, Y. H.; Liu, J. L.; Wang, K. L. Band alignments and photon-induced carrier transfer from wetting layers to Ge islands grown on Si(001). *Appl. Phys. Lett.* **2001**, *78*, 1763.

(26) Kamenev, B. V.; Lee, E.-K.; Chang, H.-Y.; Han, H.; Grebel, H.; Tsybeskov, L.; Kamins, T. I. Excitation-dependent photoluminescence in Ge/Si Stranski-Krastanov nanostructures. *Appl. Phys. Lett.* **2006**, *89*, 153106.

(27) Lee, E.-K.; Tsybeskov, L.; Kamins, T. I. Photoluminescence thermal quenching in three-dimensional multilayer Si/SiGe nanostructures. *Appl. Phys. Lett.* **2008**, *92*, 033110.

(28) Pezzoli, F.; Isa, F.; Isella, G.; Falub, C. V.; Kreiliger, T.; Salvalaglio, M.; Bergamaschini, R.; Grilli, E.; Guzzi, M.; von Känel, H.; Miglio, L. Ge crystals on Si show their light. *Phys. Rev. Appl.* **2014**, *1*, 044005.

(29) Gallagher, J. D.; Senaratne, C. L.; Xu, C.; Sims, P.; Aoki, T.; Smith, D. J.; Menendez, J.; Kouvetakis, J. Non-radiative recombination in Ge1-ySny light emitting diodes: The role of strain relaxation in tuned heterostructure designs. *J. Appl. Phys.* **2015**, *117*, 245704.

(30) Zelazna, K.; Polak, M. P.; Scharoch, P.; Serafinczuk, J.; Gladysiewicz, M.; Misiewicz, J.; Dekoster, J.; Kudrawiec, R. Electronic band structure of compressively strained Ge1-xSnx with $x < 0.11$




DOI: 10.1021/acsphotonics.6b00438
*ACS Photonics* 2016, 3, 2004−2009

studied by contactless electroreflectance. *Appl. Phys. Lett.* **2015**, *106*, 142102.
(31) Zelazna, K.; Welna, M.; Misiewicz, J.; Dekoster, J.; Kudrawiec, R. Temperature dependence of energy gap of Ge1-xSnx alloys with $x < 0.11$ studied by photoreflectance. *J. Phys. D: Appl. Phys.* **2016**, *49*, 235301.
(32) Vitiello, E.; Virgilio, M.; Giorgioni, A.; Frigerio, J.; Gatti, E.; Cesari, S. D.; Bonera, E.; Grilli, E.; Isella, G.; Pezzoli, F. Spin-dependent direct gap emission in tensile-strained Ge films on Si substrates. *Phys. Rev. B: Condens. Matter Mater. Phys.* **2015**, *92*, 201203.
(33) Pezzoli, F.; Qing, L.; Giorgioni, A.; Isella, G.; Grilli, E.; Guzzi, M.; Dery, H. Spin and energy relaxation in germanium studied by spin-polarized direct-gap photoluminescence. *Phys. Rev. B: Condens. Matter Mater. Phys.* **2013**, *88*, 045204.
(34) Pezzoli, F.; Giorgioni, A.; Gallacher, K.; Isa, F.; Biagioni, P.; Millar, R. W.; Gatti, E.; Grilli, E.; Bonera, E.; Isella, G.; Paul, D. J.; Miglio, L. Disentangling nonradiative recombination processes in Ge micro-crystals on Si substrates. *Appl. Phys. Lett.* **2016**, *108*, 262103.
(35) Reshchikov, M. A. Temperature dependence of defect-related photoluminescence in III-V and II-VI semiconductors. *J. Appl. Phys.* **2014**, *115*, 012010.
(36) Figielski, T. Recombination at dislocations. *Solid-State Electron.* **1978**, *21*, 1403.



DOI: 10.1021/acsphotonics.6b00438
*ACS Photonics* 2016, 3, 2004−2009